

# A geometric measurement of $H_0$ by the Megamaser Cosmology Project

Dom Pesce

In collaboration with: Jim Braatz (PI), Mark Reid, Jim Condon,  
Feng Gao, Christian Henkel, Violette Impellizzeri, Cheng-Yu Kuo,  
Anca Constantin, Jenny Greene, Lei Hao, Adam Riess, Dan  
Scolnic, Fred Lo

September 10, 2022

*Tensions in cosmology – Corfu*

CENTER FOR **ASTROPHYSICS**  
HARVARD & SMITHSONIAN

Image credit: Sophia Dagnello, NRAO/AUI/NSF



# Astrophysical H<sub>2</sub>O megamasers

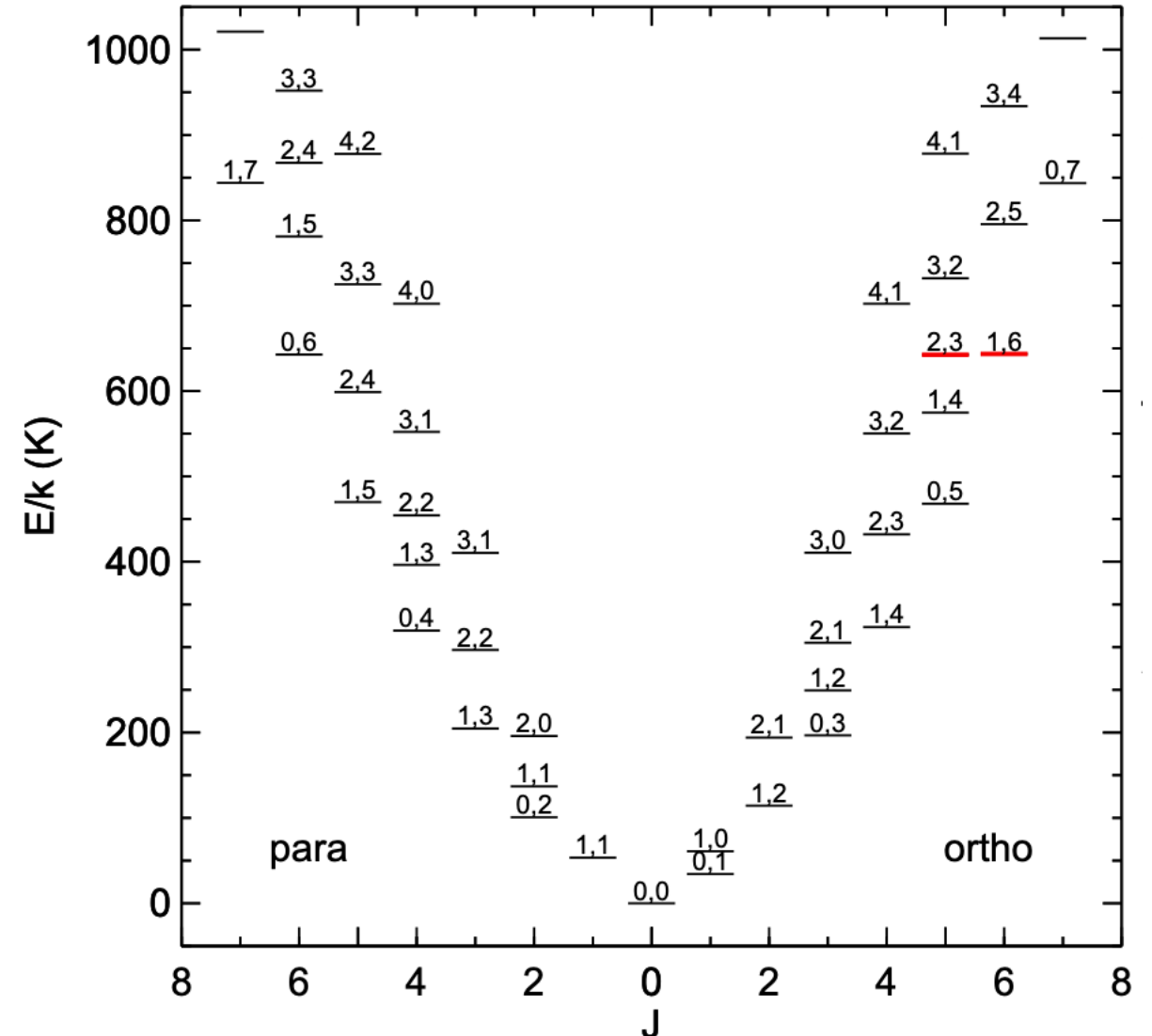


The warm ( $T \approx 1000$  K), dense ( $n \approx 10^9$  cm<sup>-3</sup>) molecular gas in AGN accretion disks on  $\sim$ pc scales contains water

One rotational transition of the water molecule, with a rest frequency of  $\sim$ 22 GHz, can sustain maser emission under these physical conditions

The name “megamaser” comes from their large luminosities:

- Galactic masers  $L \lesssim 10^{-4} L_{\odot}$
- Megamasers  $L \gtrsim 10^2 L_{\odot}$



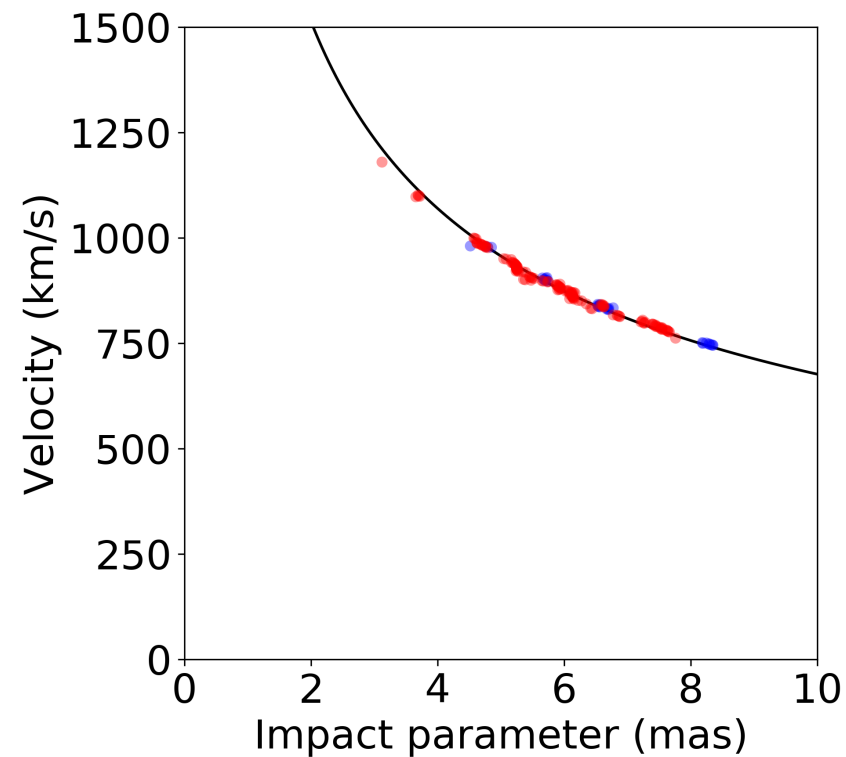
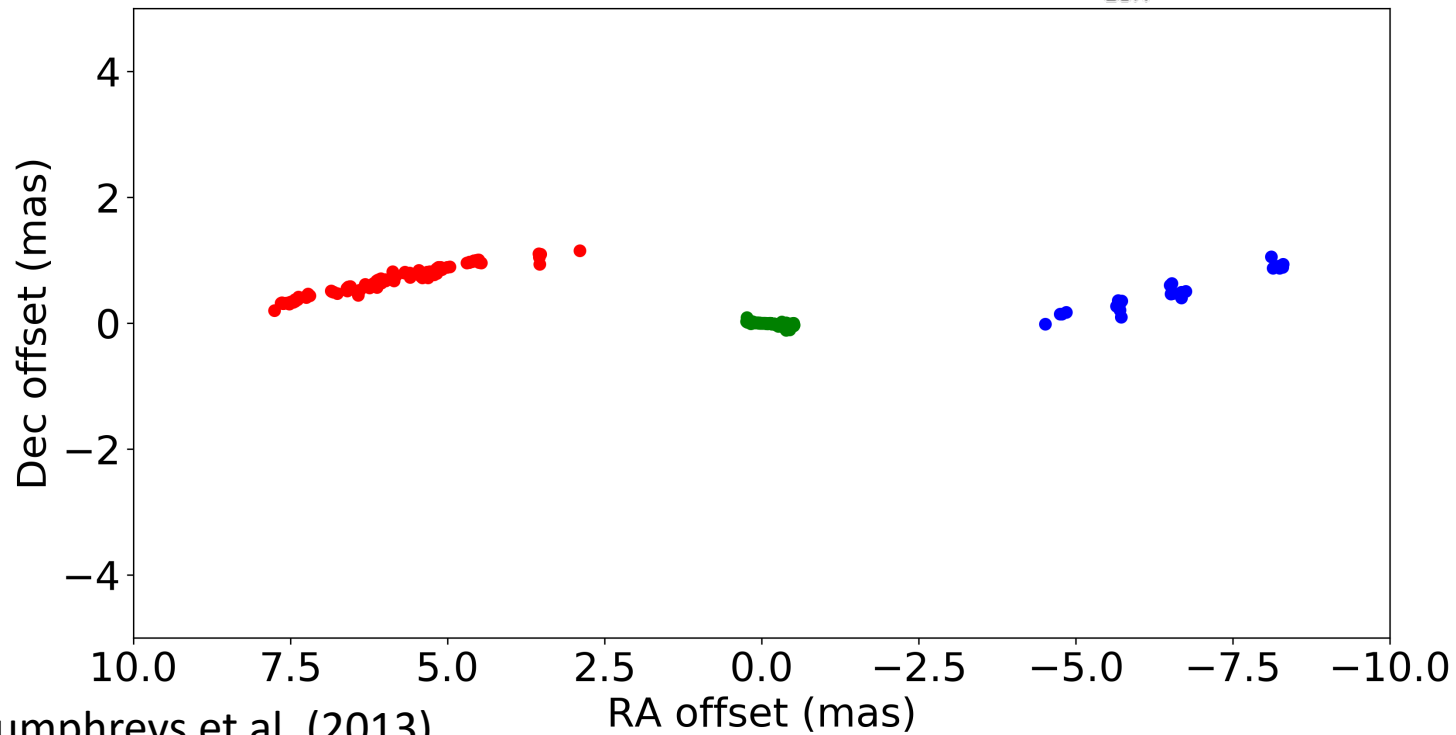
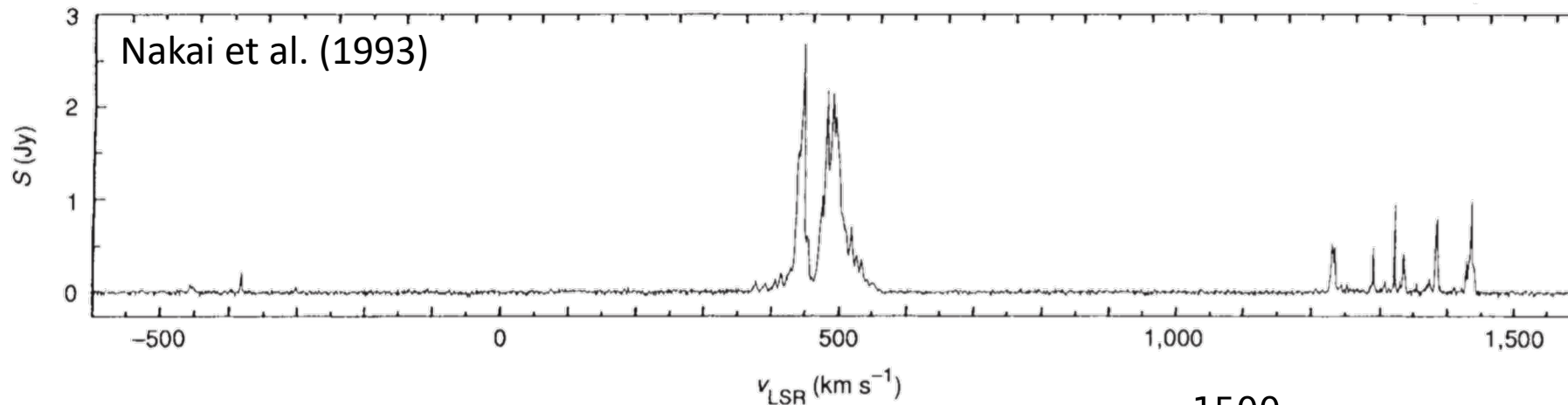
# Two primary cosmological uses for megamasers

---



1. Nearby systems for which high-precision distance measurements can be made are useful as extragalactic anchors for distance ladder methods
  - currently, only NGC 4258 is used for this purpose
2. All maser systems – but particularly the more distant ones – provide one-step geometric  $H_0$  measurements in the local universe, independent of distance ladders
  - alternatively, megamasers are a “one rung” distance ladder

# NGC 4258 – the original megamaser galaxy



# NGC 4258 – the original megamaser galaxy



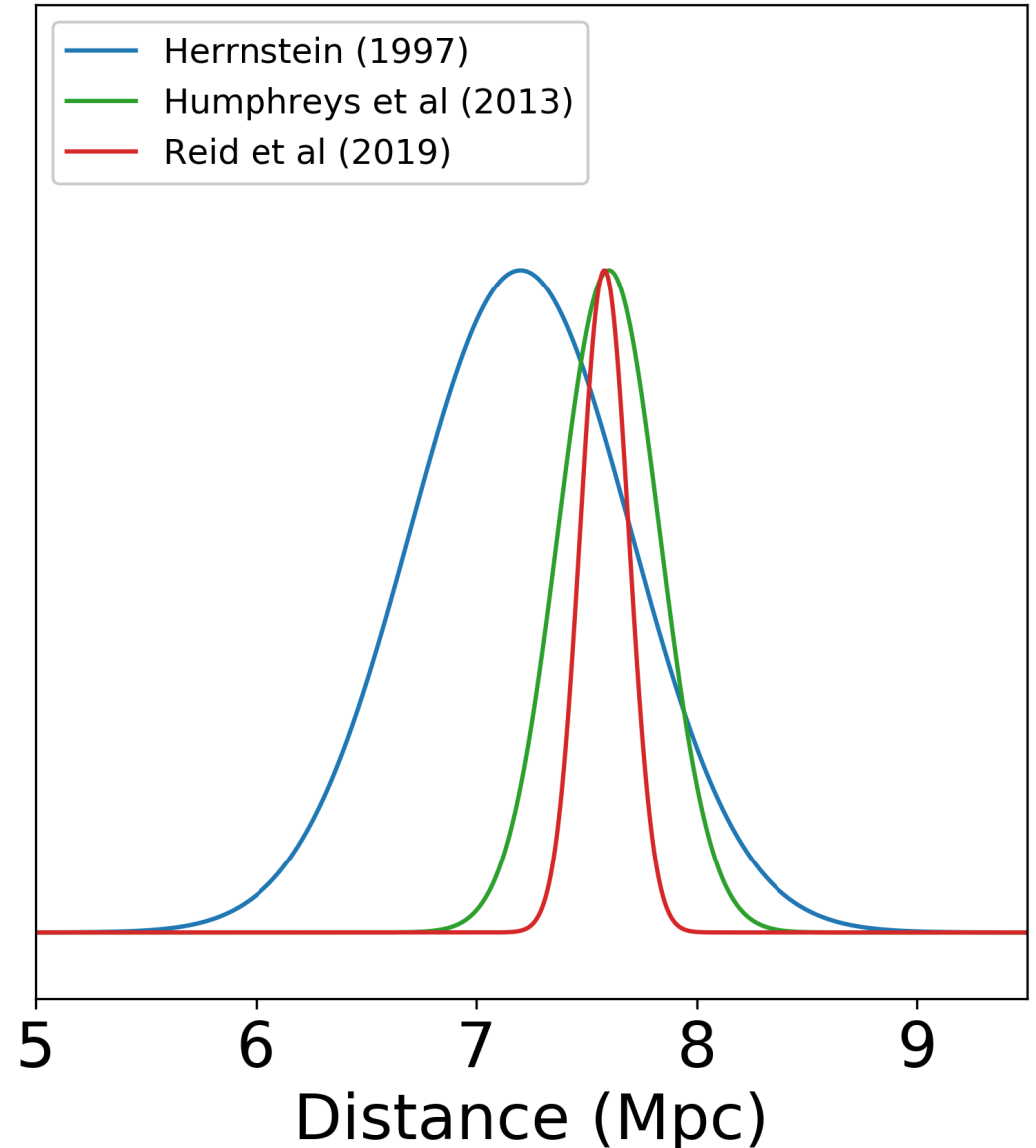
The galaxy NGC 4258 hosts the first discovered disk megamaser system

First observed by Claussen et al. (1984); breakthrough in understanding with Nakai et al. (1993)

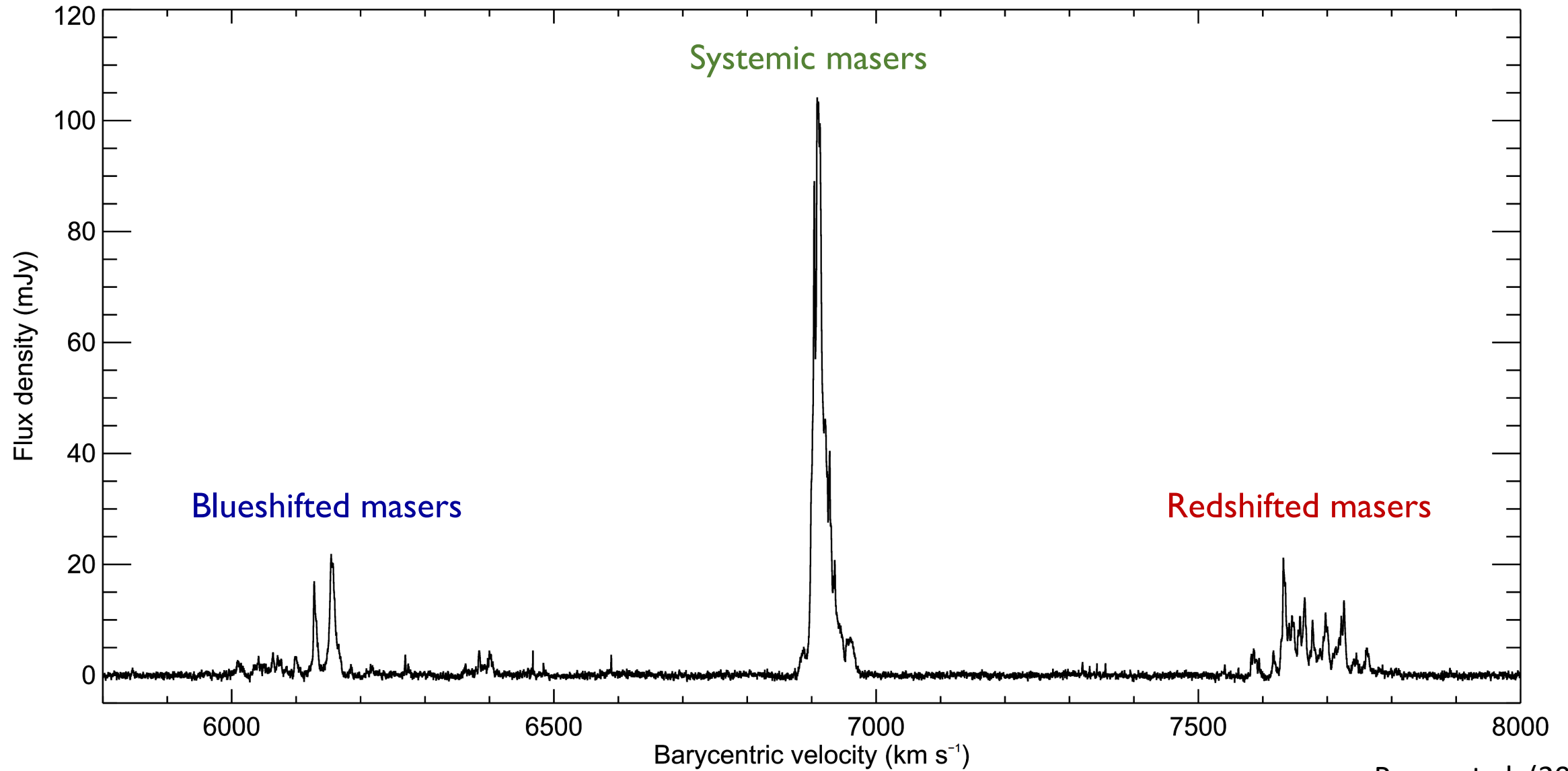
VLBI maps of the system reveal an orderly distribution of maser spots, which trace out a nearly perfect Keplerian rotation curve

Detailed modeling of the maser disk in this system has resulted in a distance constraint with a  $\sim 1.5\%$  precision

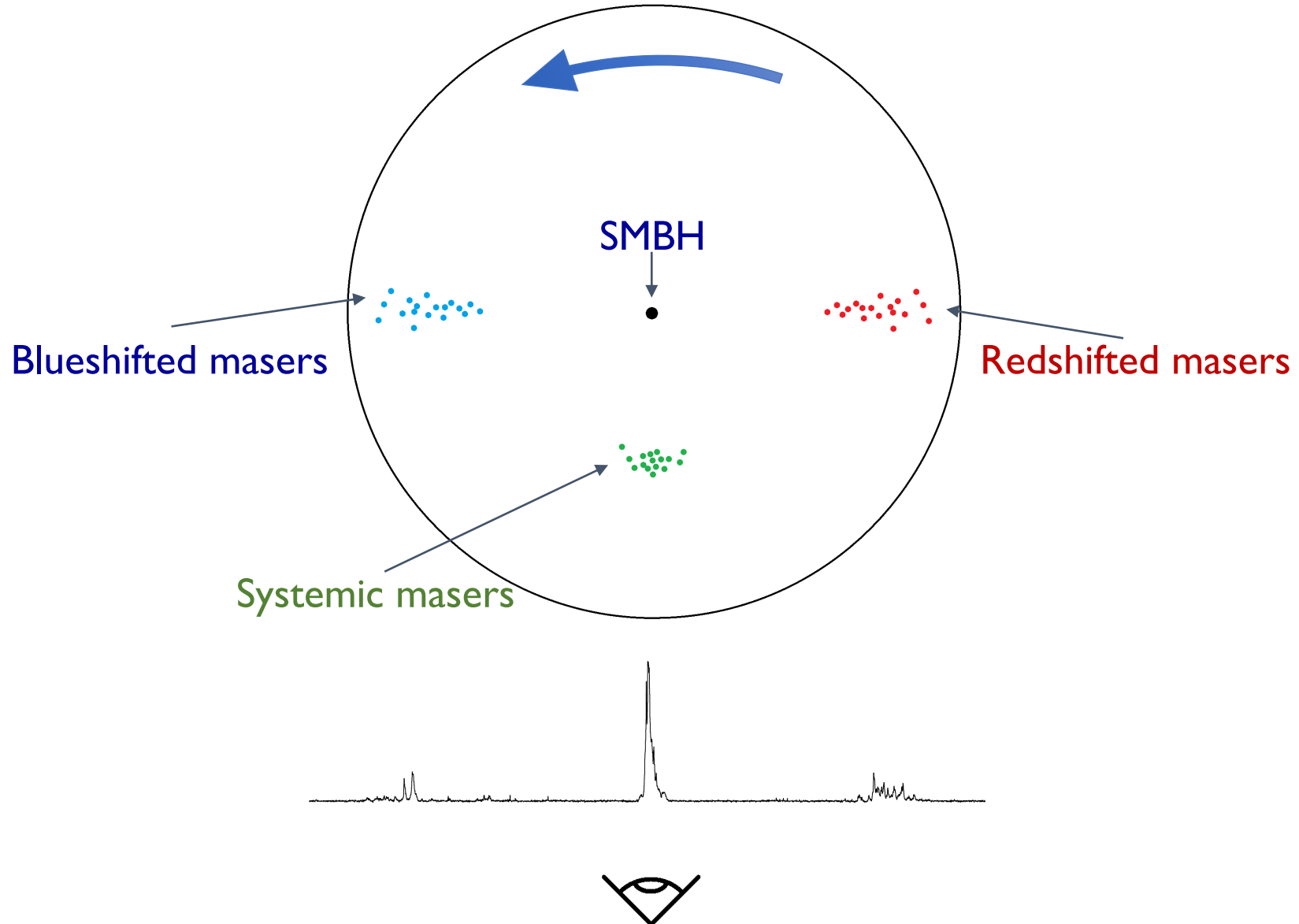
- limited by systematics associated with our understanding of the geometry and kinematics of the accretion disk



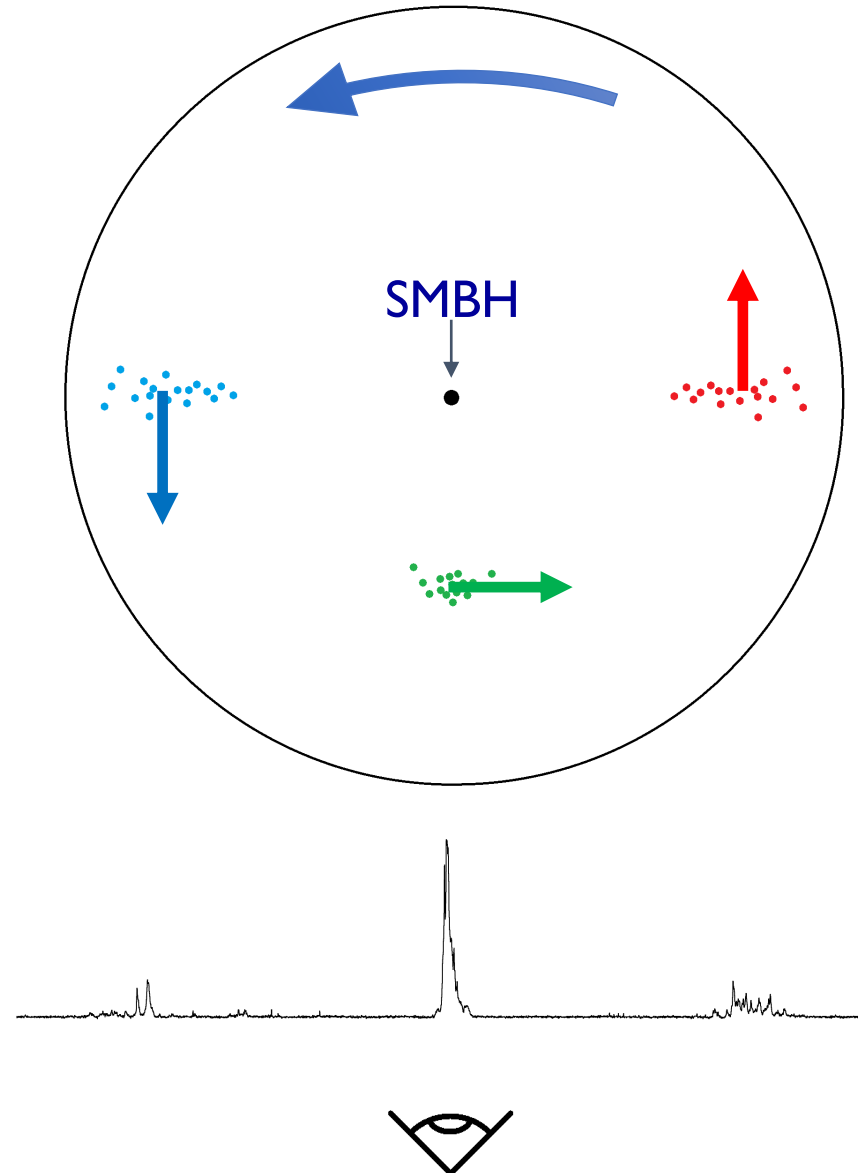
# Disk masers – basic model



# Disk masers – basic model

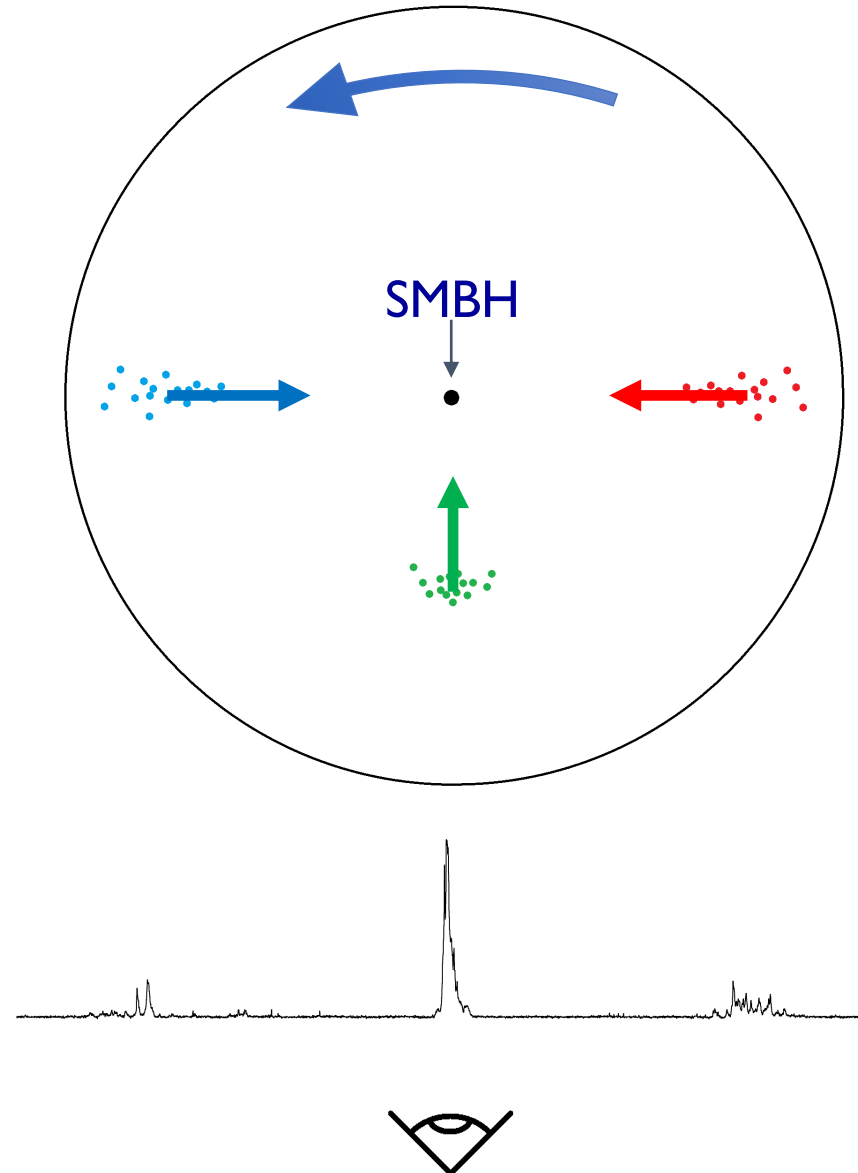


velocity  
vectors





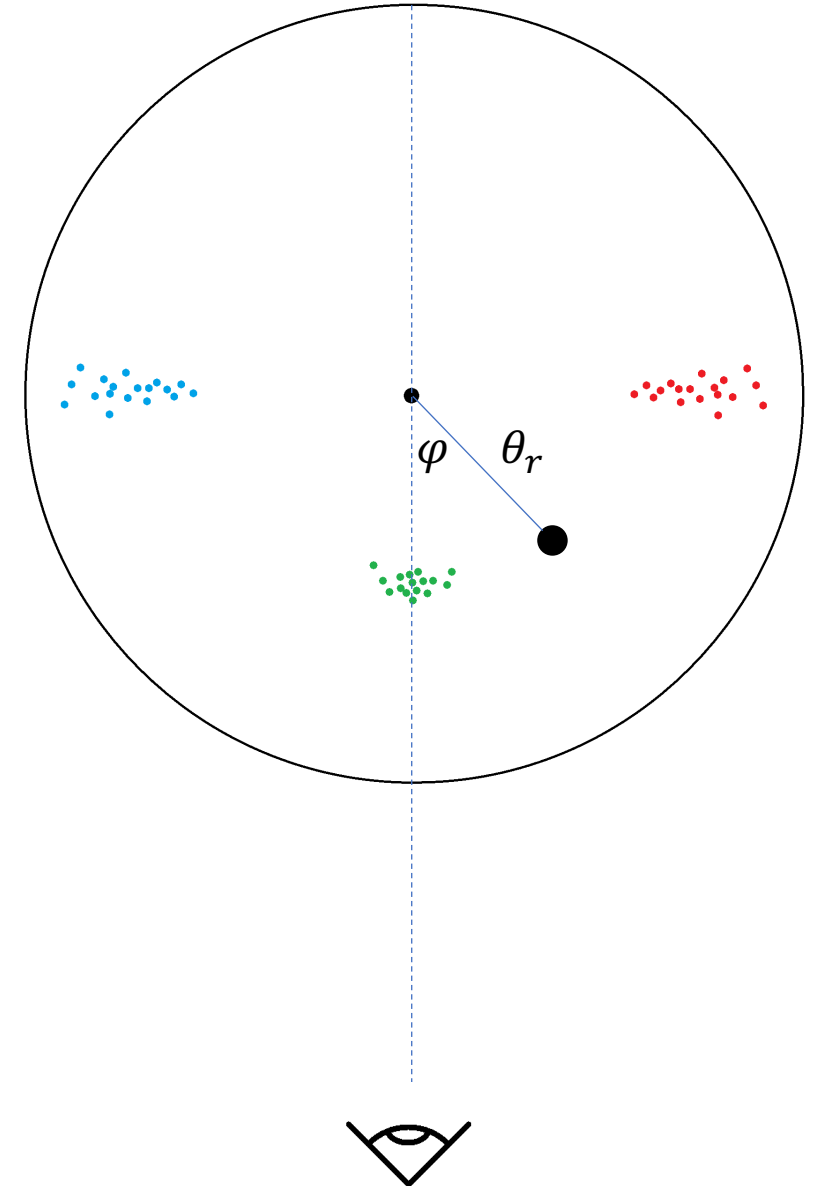
acceleration  
vectors



# Disk masers – basic model



Consider a masing cloud on a circular orbit at (angular) radius  $\theta_r$  around a central SMBH of mass  $M$  and situated at an azimuthal angle  $\varphi$  with respect to the line of sight



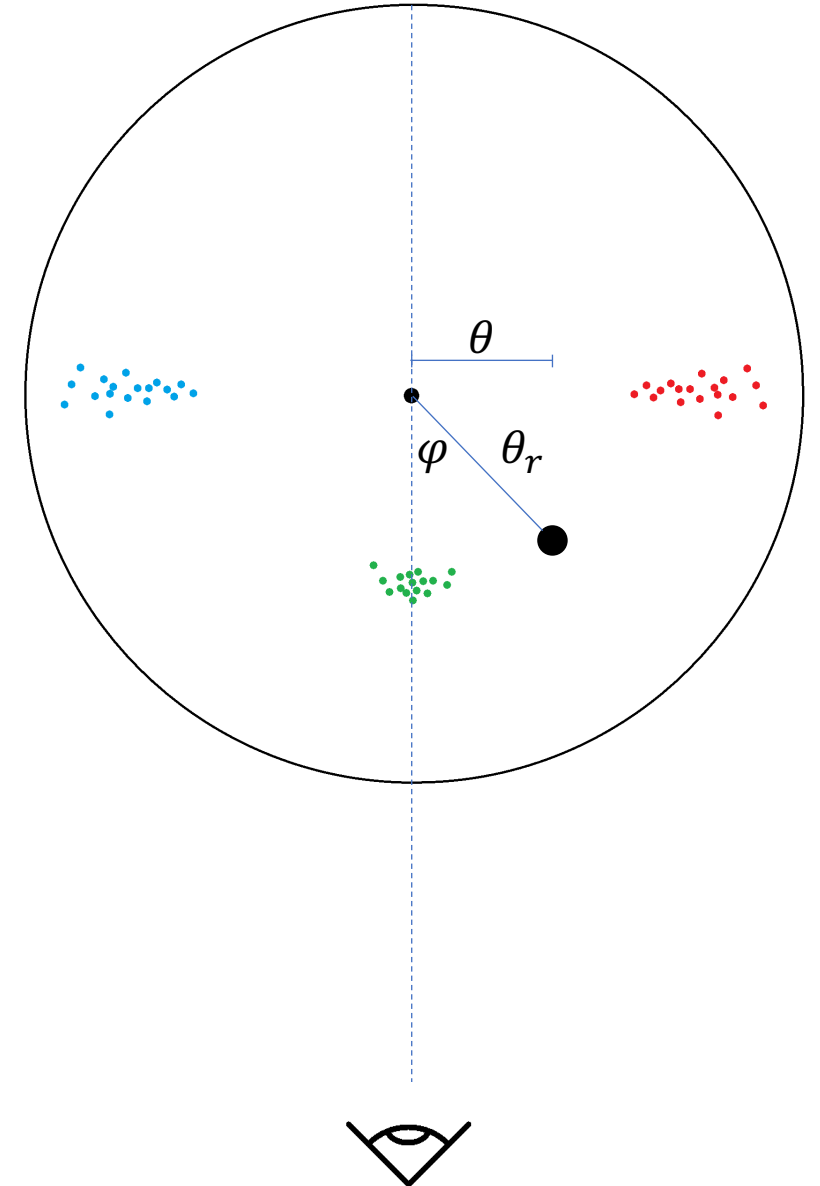
# Disk masers – basic model



Consider a masing cloud on a circular orbit at (angular) radius  $\theta_r$  around a central SMBH of mass  $M$  and situated at an azimuthal angle  $\varphi$  with respect to the line of sight

Observed (on-sky) position:

$$\theta = \theta_r \sin(\varphi)$$



# Disk masers – basic model

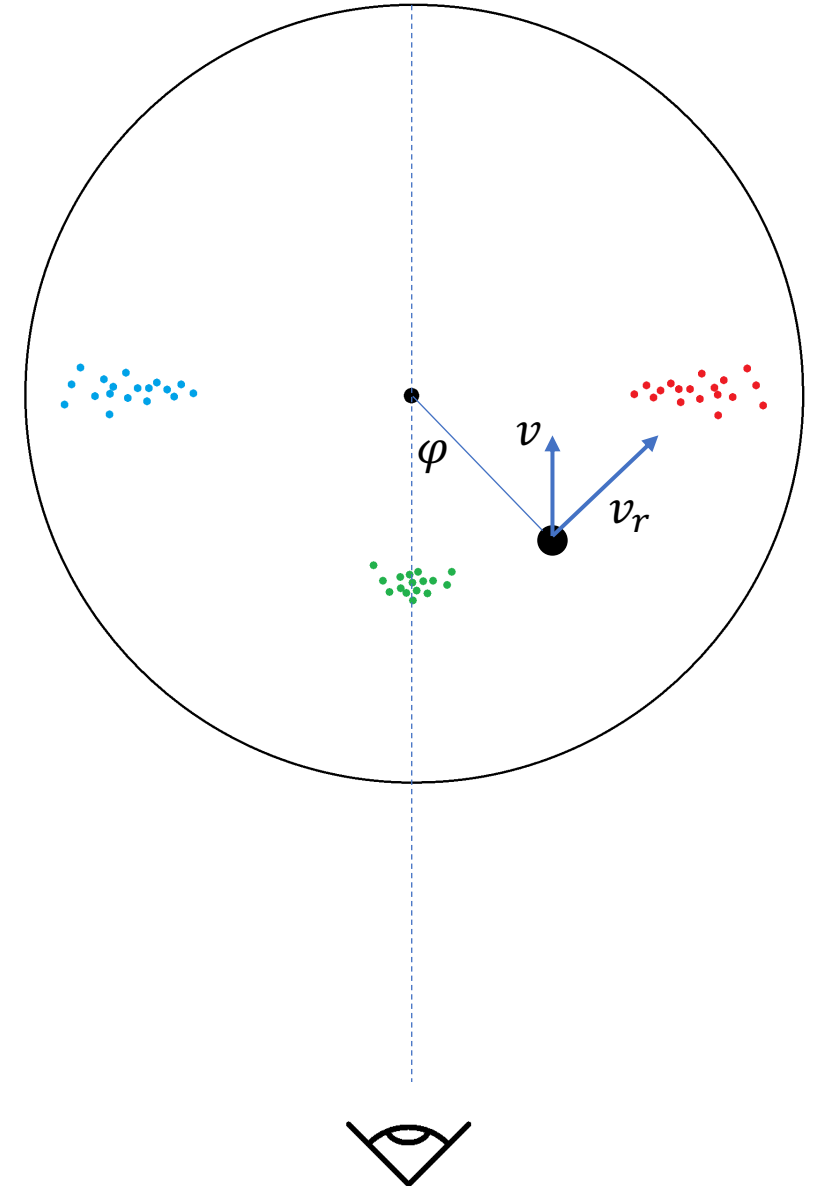


Consider a masing cloud on a circular orbit at (angular) radius  $\theta_r$  around a central SMBH of mass  $M$  and situated at an azimuthal angle  $\varphi$  with respect to the line of sight

Observed (on-sky) position:  $\theta = \theta_r \sin(\varphi)$

Observed (line-of-sight) velocity:  $v = v_r \sin(\varphi)$

$$v_r = \sqrt{\frac{GM}{\theta_r D}}$$



# Disk masers – basic model



Consider a masing cloud on a circular orbit at (angular) radius  $\theta_r$  around a central SMBH of mass  $M$  and situated at an azimuthal angle  $\varphi$  with respect to the line of sight

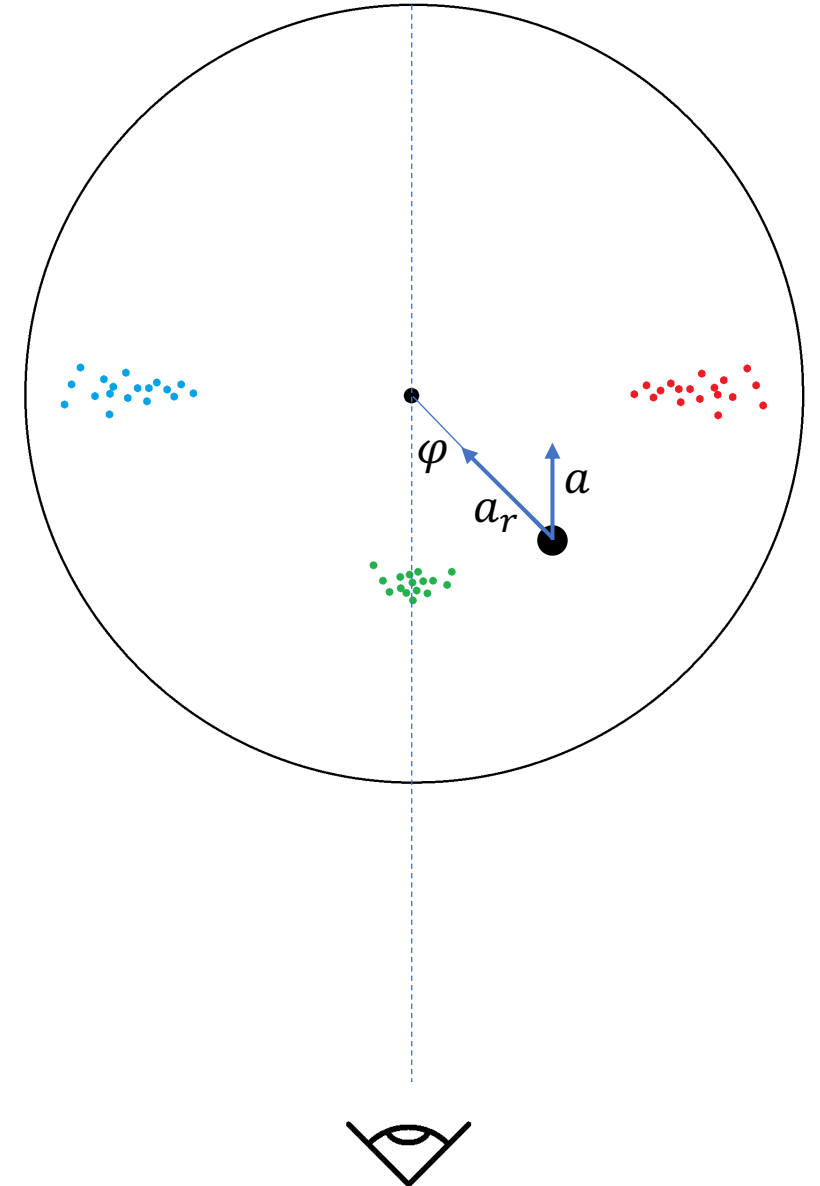
Observed (on-sky) position:  $\theta = \theta_r \sin(\varphi)$

Observed (line-of-sight) velocity:  $v = v_r \sin(\varphi)$

Observed (line-of-sight) acceleration:  $a = a_r \cos(\varphi)$

$$v_r = \sqrt{\frac{GM}{\theta_r D}}$$

$$a_r = \frac{v_r^2}{\theta_r D} = \frac{GM}{\theta_r^2 D^2}$$



# Disk masers – basic model




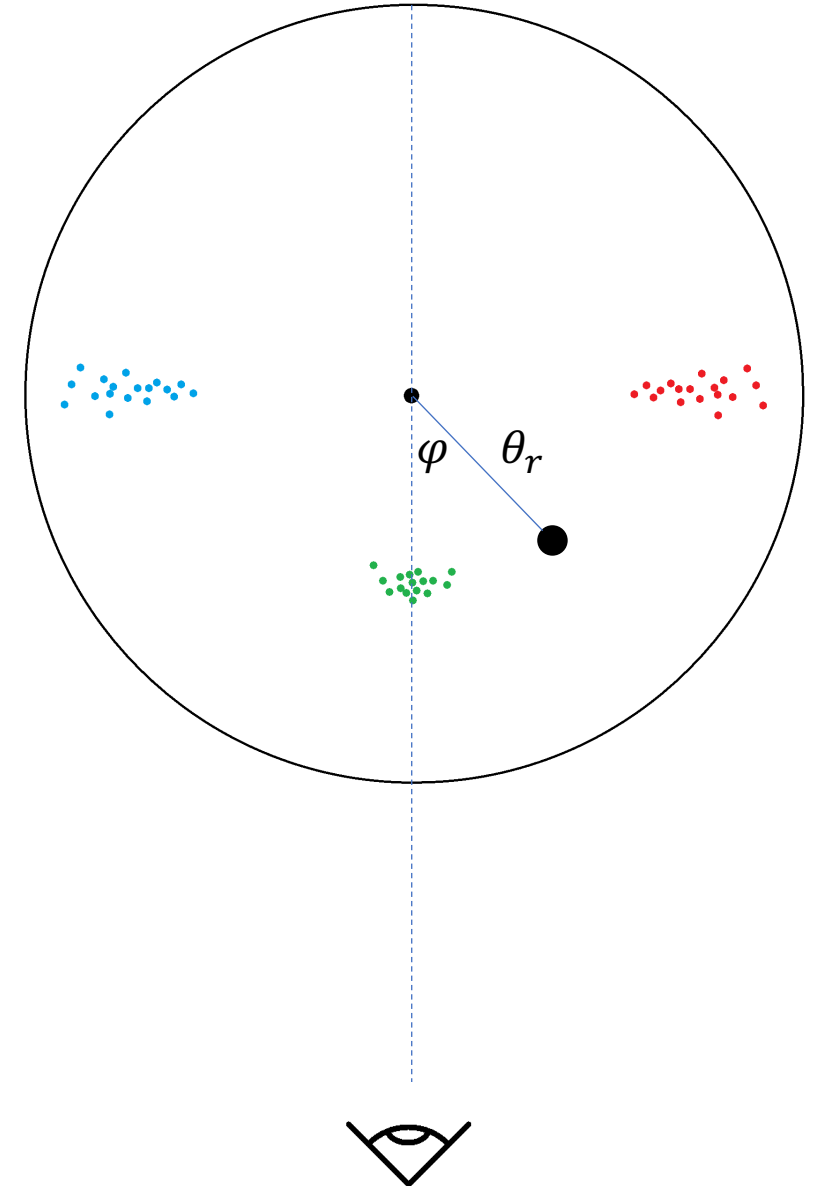
Consider a masing cloud on a circular orbit at (angular) radius  $\theta_r$  around a central SMBH of mass  $M$  and situated at an azimuthal angle  $\varphi$  with respect to the line of sight

Observed (on-sky) position:  $\theta = \theta_r \sin(\varphi)$   
Observed (line-of-sight) velocity:  $v = v_r \sin(\varphi)$   
Observed (line-of-sight) acceleration:  $a = a_r \cos(\varphi)$

$$v_r = \sqrt{\frac{GM}{\theta_r D}}$$
$$a_r = \frac{v_r^2}{\theta_r D} = \frac{GM}{\theta_r^2 D^2}$$

 = measured

 = fit



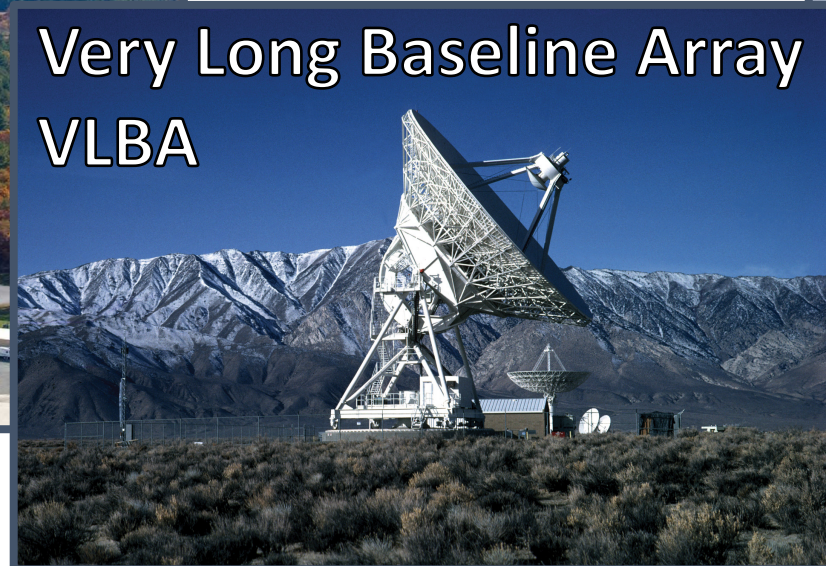
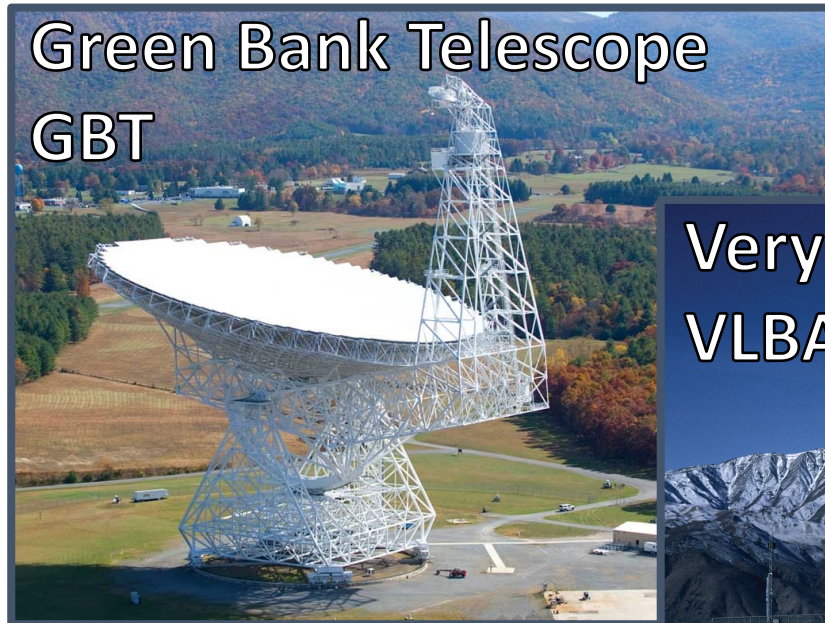
# The Megamaser Cosmology Project



NGC 4258 is very nearby ( $D = 7.6$  Mpc), but other megamaser-hosting galaxies are located much farther away and participate in the Hubble flow

- By measuring distances to these galaxies, we can directly constrain the Hubble constant,  $H_0$

The **Megamaser Cosmology Project** (MCP) is a multi-year effort to find megamaser-hosting galaxies and measure their distances, with the goal of measuring  $H_0$  to few-percent precision



# The Megamaser Cosmology Project: the difficulty



NGC 4258



UGC 3789



NGC 6323



CGCG 074-064



NGC 6264



NGC 5765b



0.2 pc



# The Megamaser Cosmology Project: the difficulty



NGC 4258



UGC 3789



NGC 6323



CGCG 074-064



NGC 6264



NGC 5765b



2 mas

# The Megamaser Cosmology Project: the difficulty



NGC 4258



UGC 3789



NGC 6323



CGCG 074-064



NGC 6264



NGC 5765b



Typical VLBA  
resolution element



2 mas

To date, the MCP has determined distances to 5 megamaser-hosting AGN:

- UGC 3789 (Reid et al. 2009, Braatz et al. 2010, Reid et al. 2013)
- NGC 6264 (Kuo et al. 2013)
- NGC 6323 (Kuo et al. 2015)
- NGC 5765b (Gao et al. 2016)
- CGCG 074-064 (Pesce et al. 2020a)

Because the megamaser technique also precisely determines the line-of-sight redshift of each galaxy, we can use the combined distance+redshift measurements to constrain  $H_0$

The individual distance measurements are much less precise than for NGC 4258

- must combine multiple measurements to get a good handle on  $H_0$

# MCP $H_0$ constraints



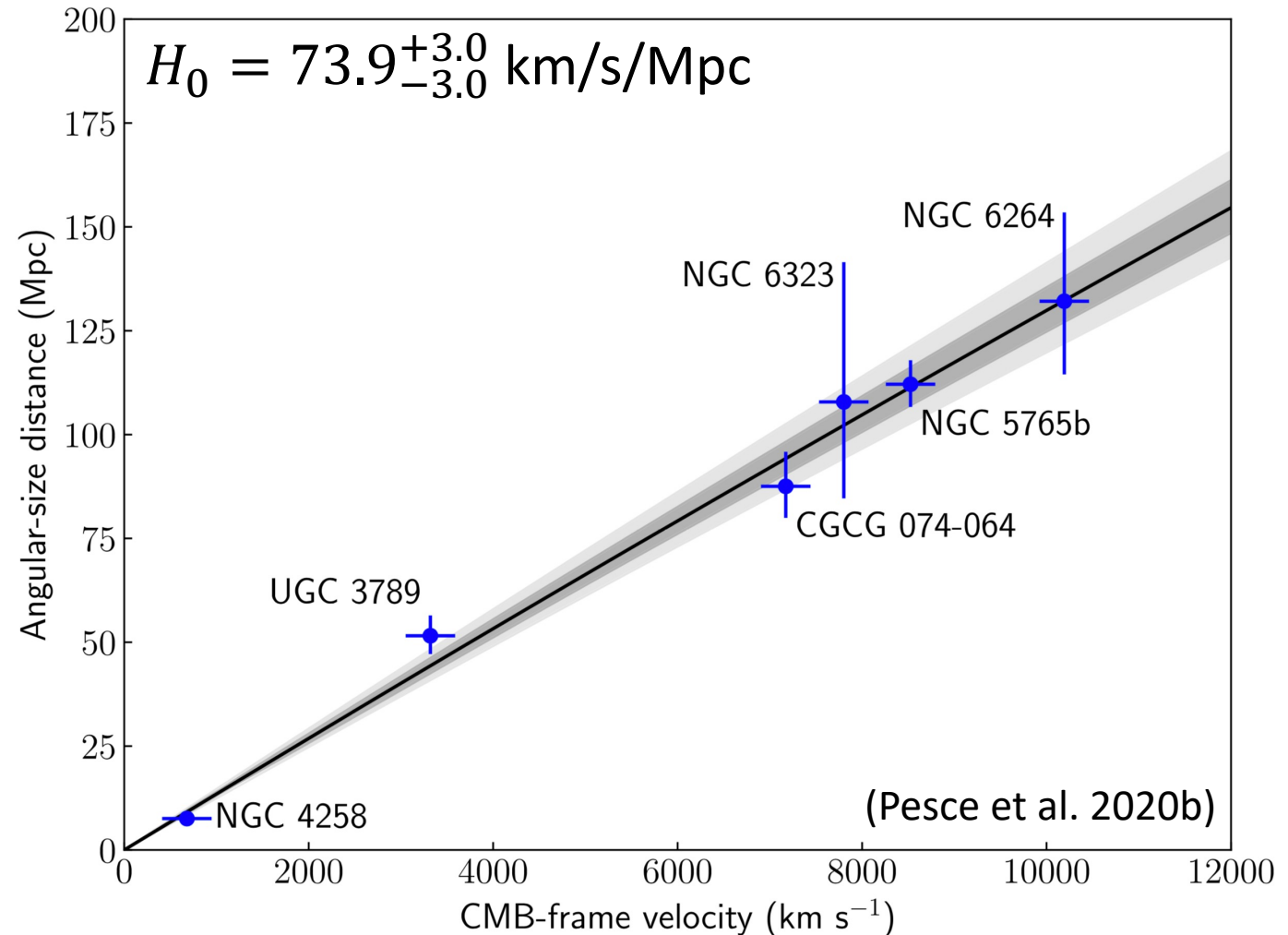
We have combined the 5 MCP targets with NGC 4258 to produce a maser-only constraint on  $H_0$

- the latest maser disk modeling formalism has been applied to each galaxy

We jointly fit the 6 distance ( $D_i$ ) and redshift ( $z_i$ ) measurements to a simple cosmological model:

$$D_i = \frac{c}{H_0(1+z_i)} \int_0^{z_i} \frac{dz}{\sqrt{\Omega_m(1+z)^3 + (1-\Omega_m)}}$$

Assuming a 250 km/s peculiar velocity uncertainty for each galaxy, we determine  $H_0 = 73.9 \pm 3.0$  km/s/Mpc

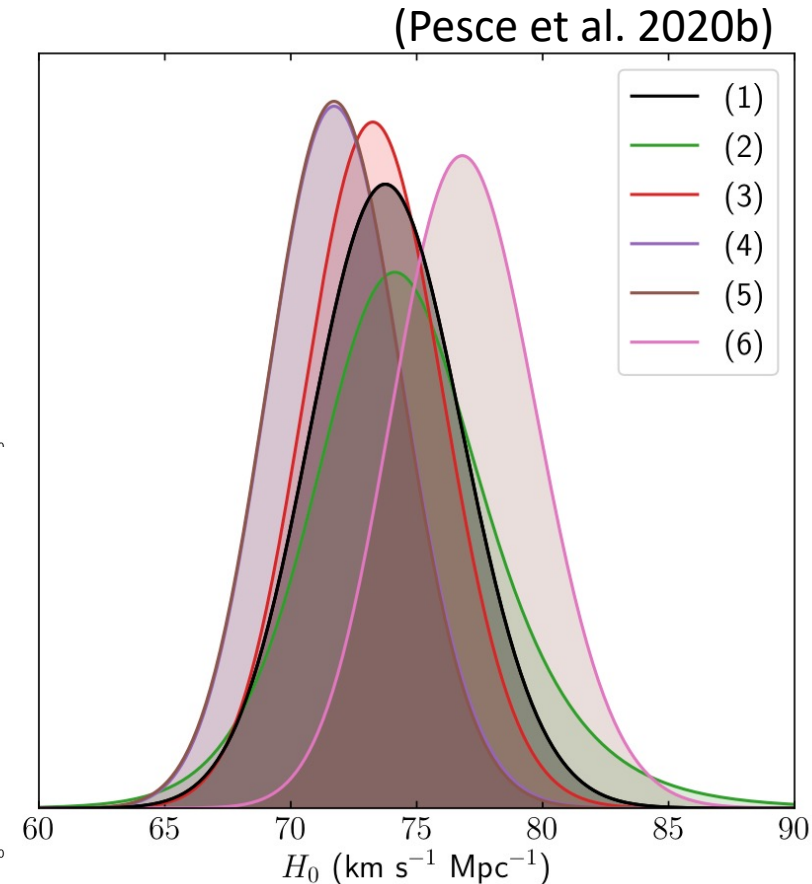
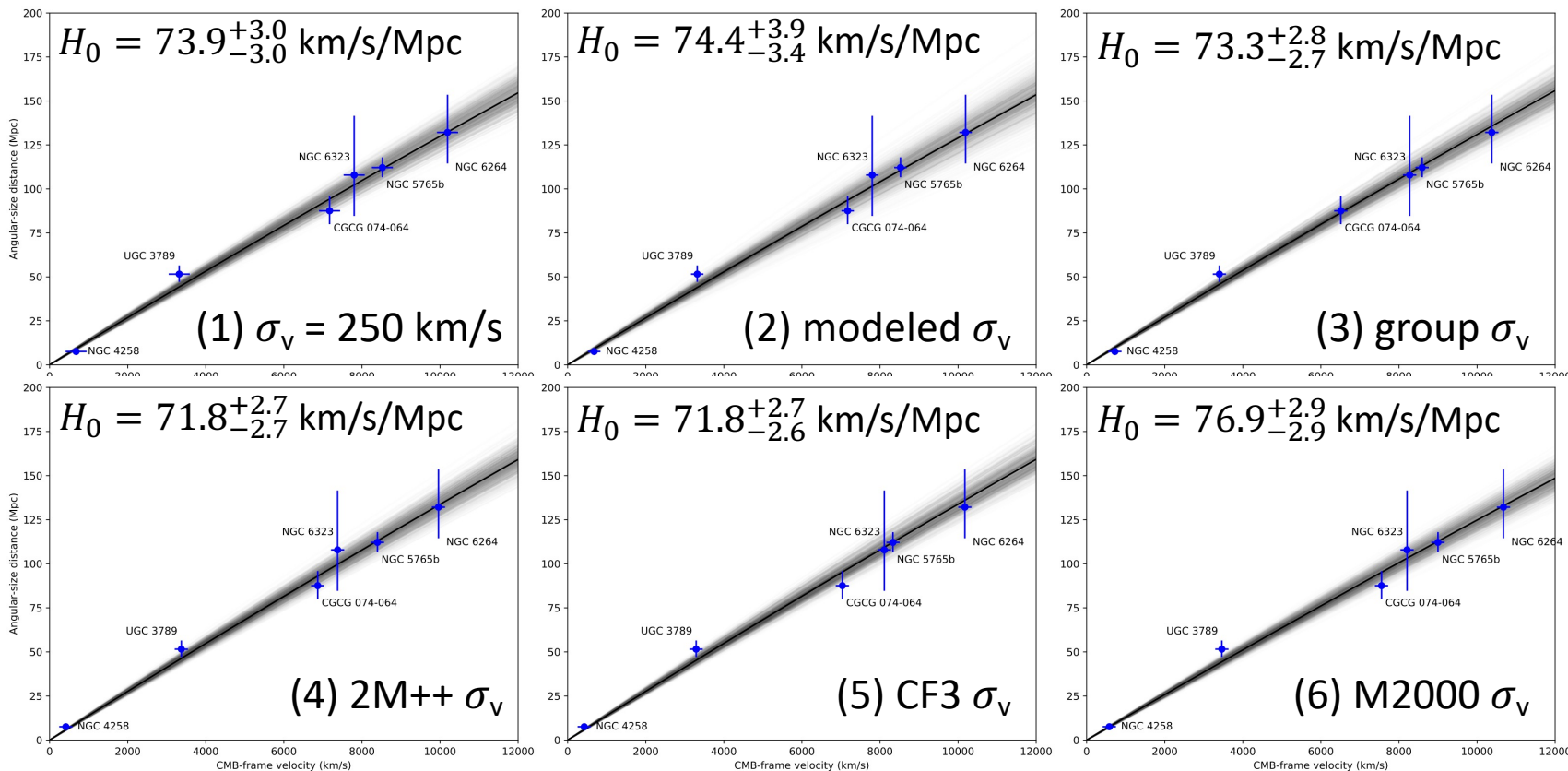


# Sources of uncertainty in MCP $H_0$ constraints



## Peculiar velocities

- Though the statistical uncertainty in each galaxy's redshift is tiny ( $\lesssim 2$  km/s), its systematic deviation from the Hubble flow is unknown
- Mitigation: explore a range of peculiar velocity prescriptions; incorporate peculiar velocities into the model as free parameters; increase sample size



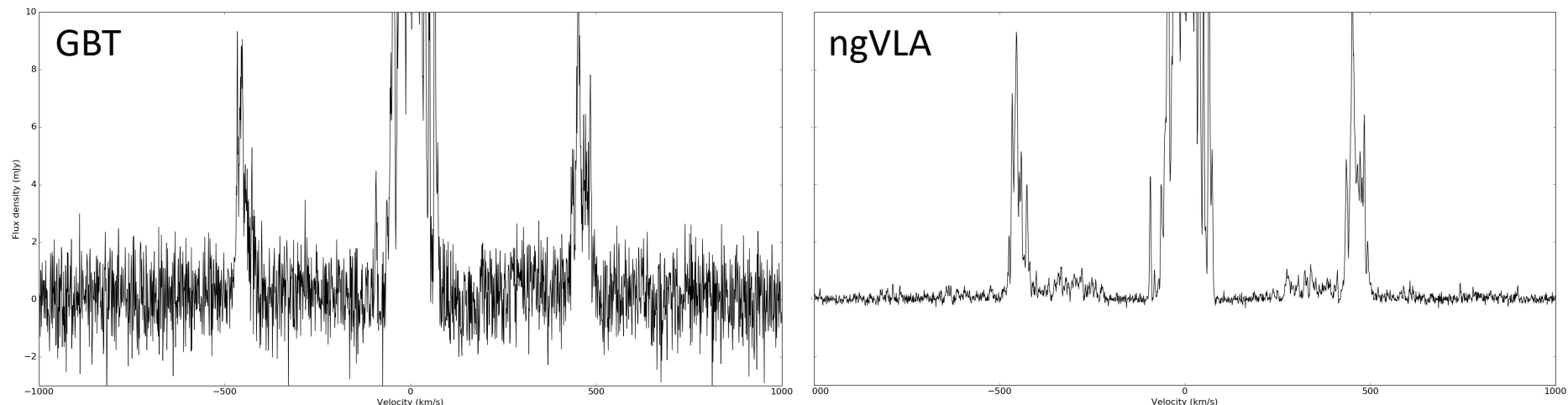
## Peculiar velocities

- Though the statistical uncertainty in each galaxy's redshift is tiny ( $\lesssim 2$  km/s), its systematic deviation from the Hubble flow is unknown
- Mitigation: explore a range of peculiar velocity prescriptions; incorporate peculiar velocities into the model as free parameters; increase sample size

## Quality of distance measurements

- Typical uncertainties in megamaser distances are  $\sim 10\%$ , compared to  $\lesssim 10^{-5}$  in redshift, and altogether they make up  $\sim 90\%$  of the  $H_0$  error budget
- Mitigation: next-generation facilities (e.g., ngVLA) operating at 22 GHz will provide  $\sim$ an order of magnitude more sensitivity in both monitoring spectra and VLBI maps

synthetic 22 GHz  
maser spectra



## Peculiar velocities

- Though the statistical uncertainty in each galaxy's redshift is tiny ( $\lesssim 2$  km/s), its systematic deviation from the Hubble flow is unknown
- Mitigation: explore a range of peculiar velocity prescriptions; incorporate peculiar velocities into the model as free parameters; increase sample size

## Quality of distance measurements

- Typical uncertainties in megamaser distances are  $\sim 10\%$ , compared to  $\lesssim 10^{-5}$  in redshift, and altogether they make up  $\sim 90\%$  of the  $H_0$  error budget
- Mitigation: next-generation facilities (e.g., ngVLA) operating at 22 GHz will provide  $\sim$ an order of magnitude more sensitivity in both monitoring spectra and VLBI maps

## Small sample size

- Currently only 6 maser sources are being used to constrain  $H_0$
- A comparable number ( $\sim 4-6$ ) have analyses ongoing
- Mitigation: leave-one-out jackknife tests; improved survey strategies are being developed (e.g., Kuo et al. 2020); next-generation facilities will see deeper and uncover fainter systems; (sub)mm water masers with ALMA (+ mm-VLBI) are being discovered and explored right now

# Future work: (sub)millimeter water masers

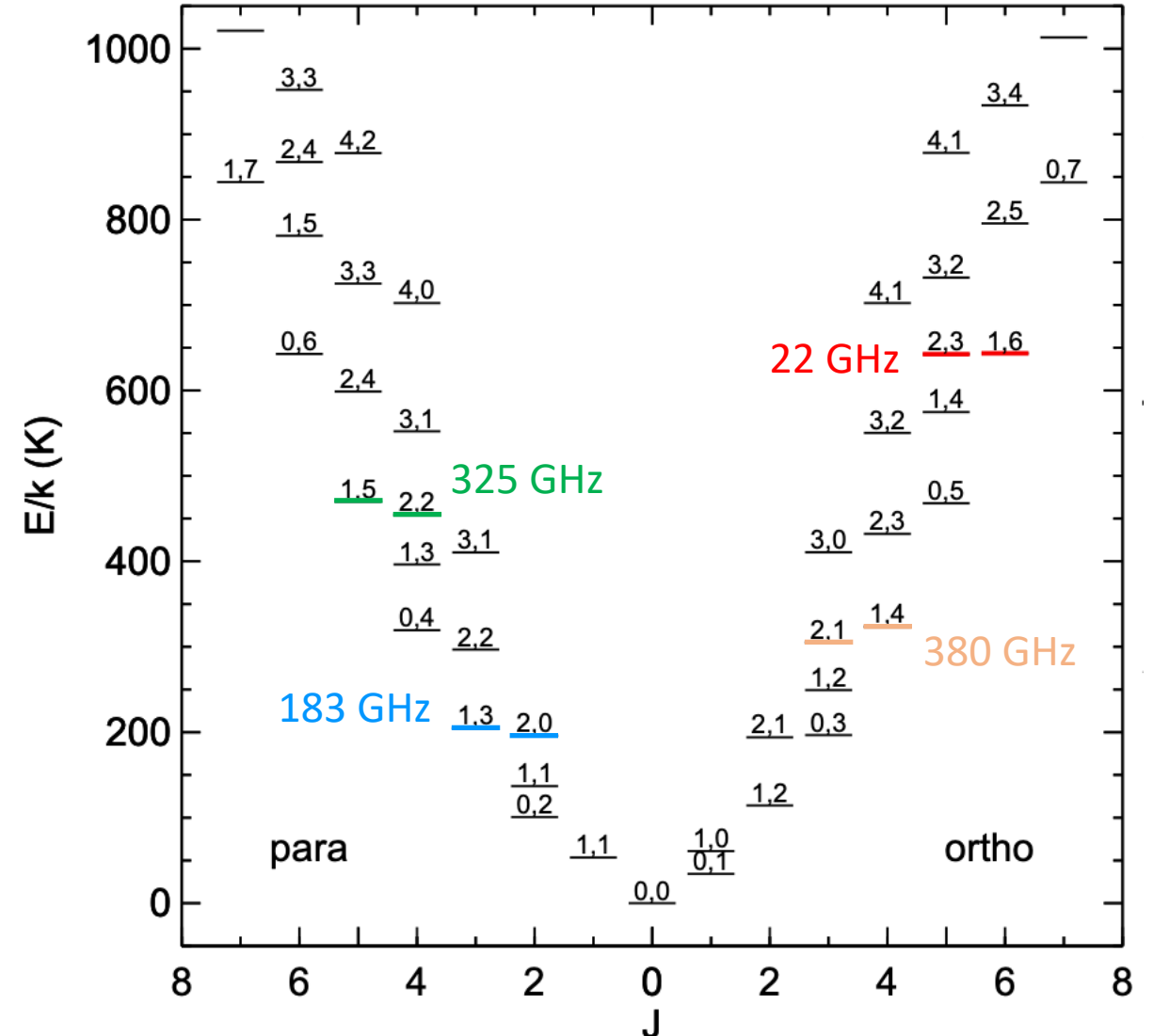


This talk has focused on the 22 GHz transition, but there are others

Future prospects for (sub)millimeter water megamaser observations using, e.g., the (ng)EHT will substantially improve the angular resolution of the VLBI maps

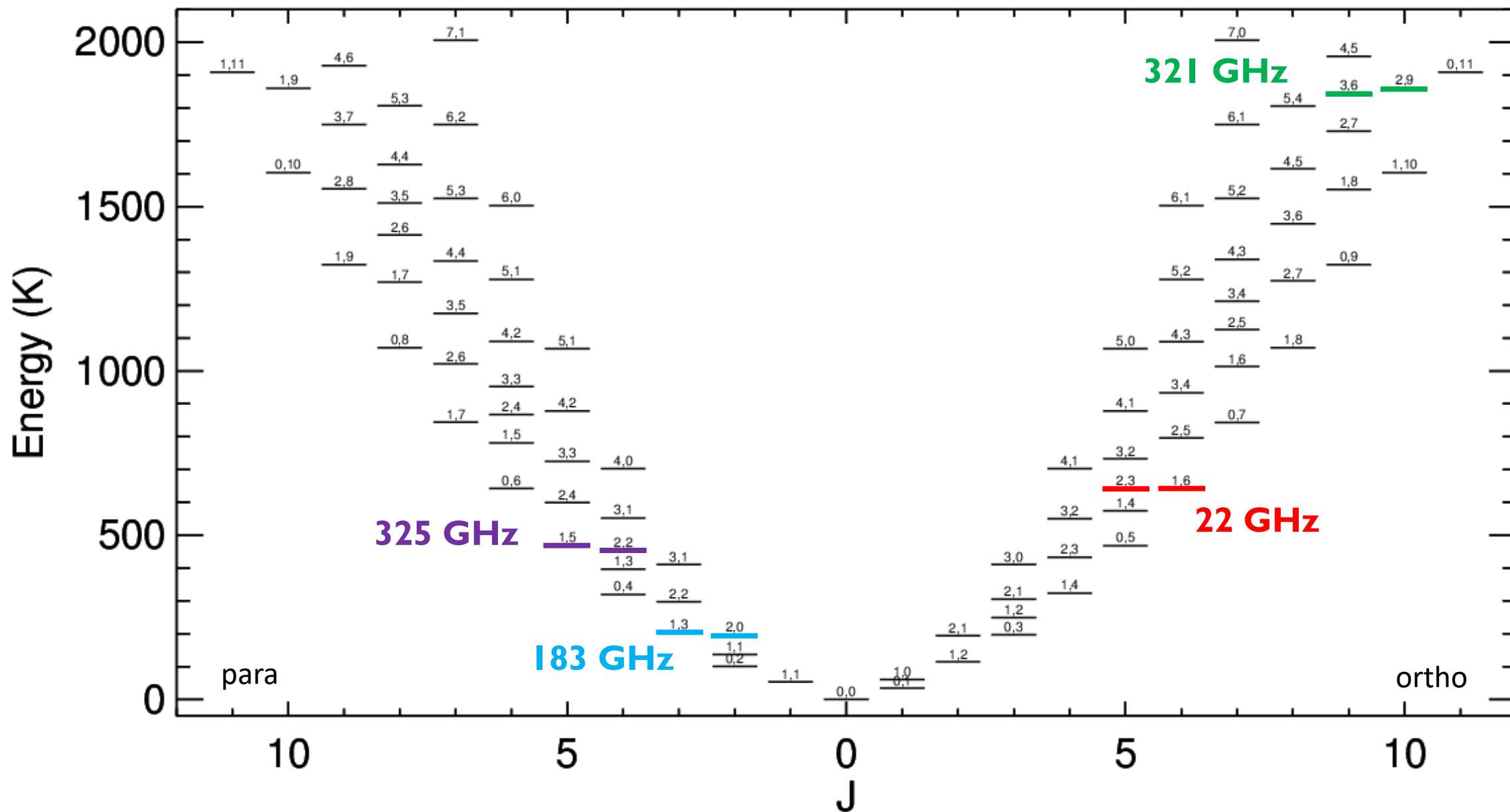
With  $\sim 10\times$  higher frequencies and similar baseline lengths, expect  $\sim 10\times$  better angular resolution

- MCP systems would be resolved at a level comparable to current NGC 4258 maps (though the sensitivity will still be lower)





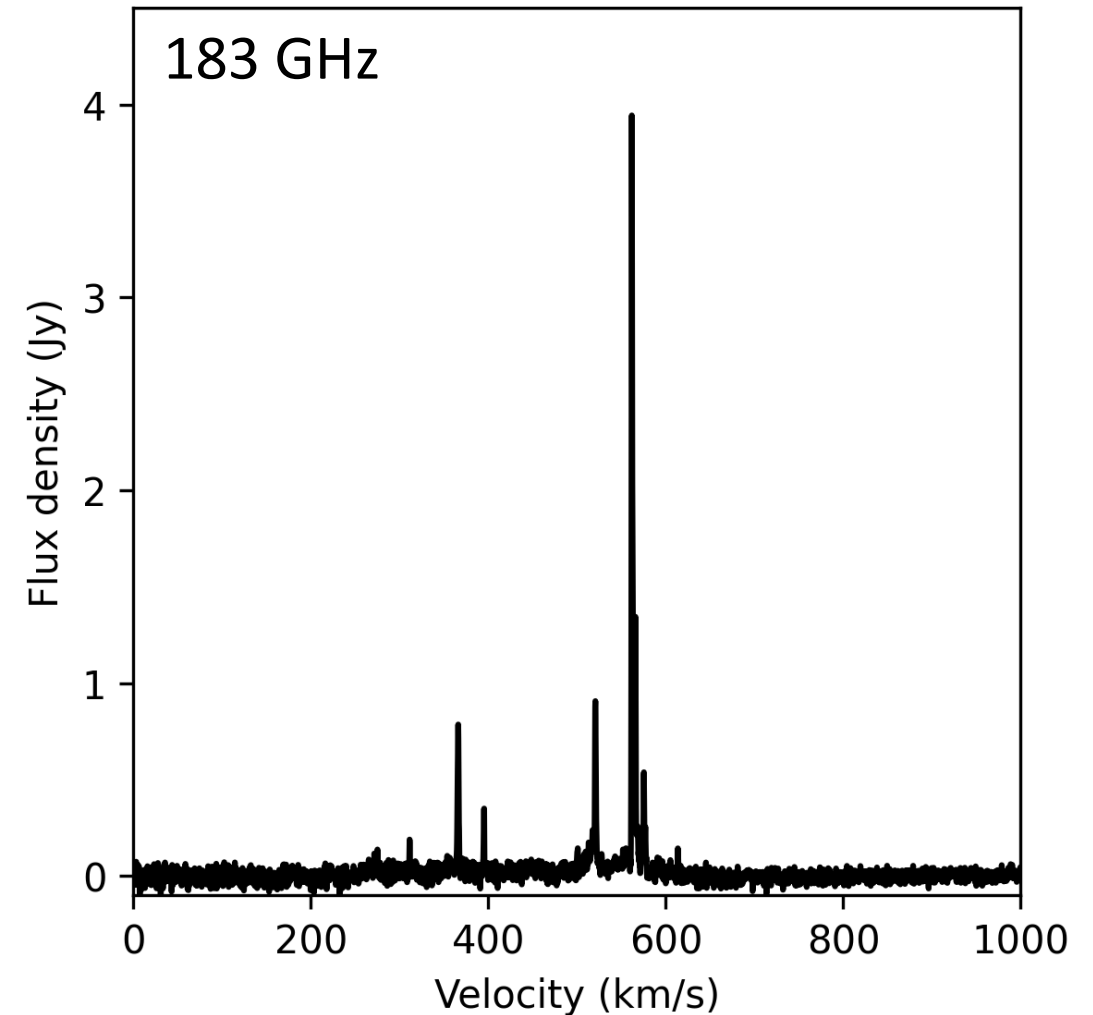
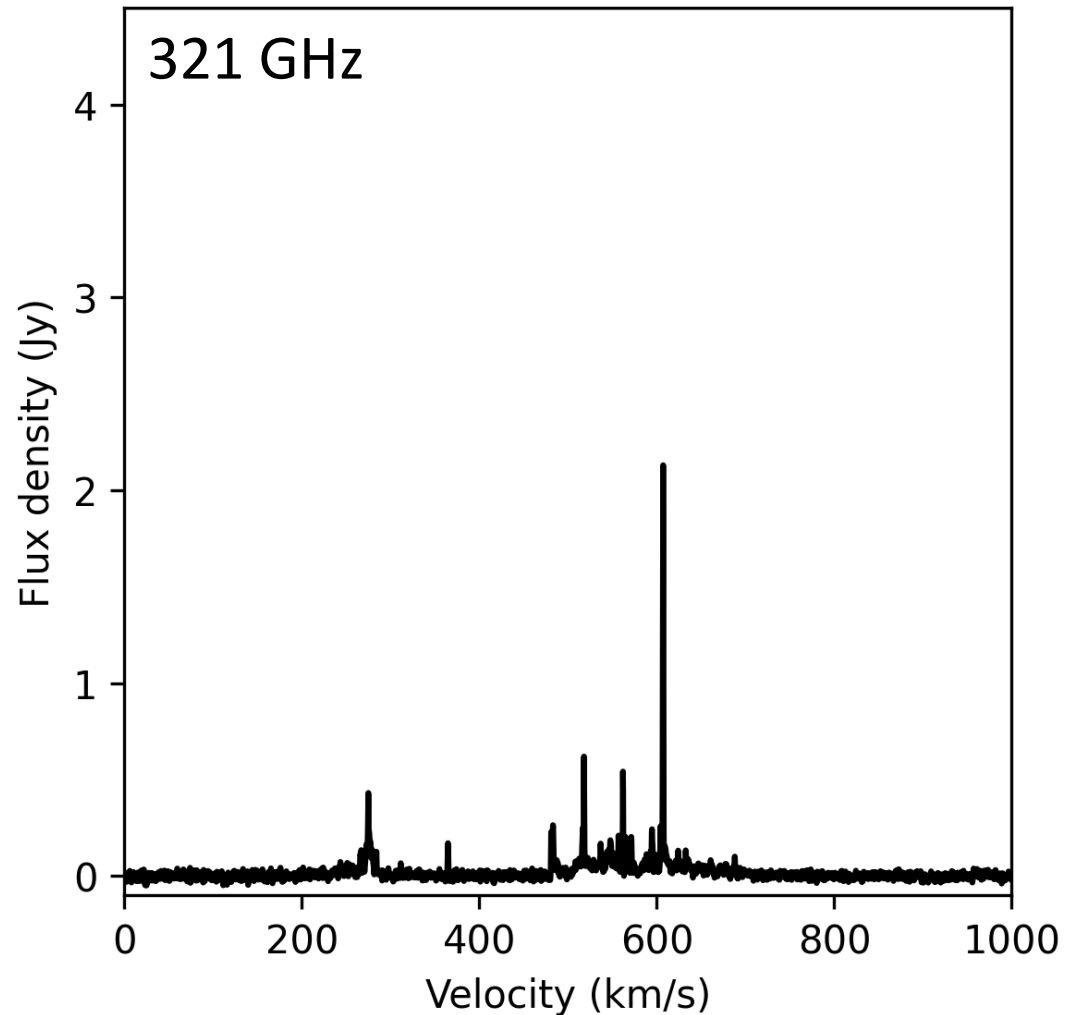
# Future work: (sub)millimeter water masers



# Future work: (sub)millimeter water masers



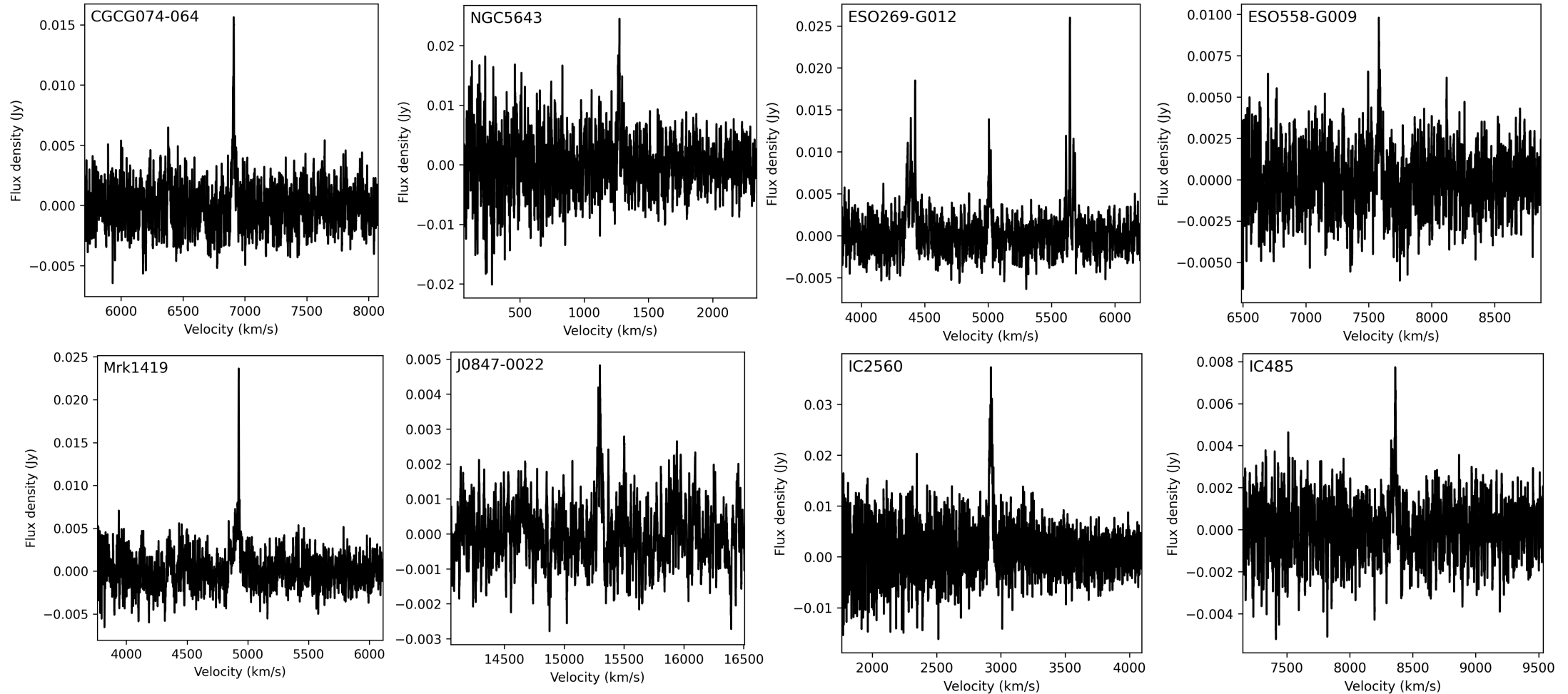
These two spectra show maser emission from the Circinus galaxy



# Future work: (sub)millimeter water masers



Initial surveys are beginning to uncover a population of AGN accretion disk megamasers emitting in these new transitions



H<sub>2</sub>O megamasers residing in AGN accretion disks provide unique and valuable tools for measuring the distances to their host galaxies

The Megamaser Cosmology Project (MCP) has discovered and determined distances towards 5 megamaser-hosting AGN

We have improved the maser disk modeling and applied the new scheme uniformly to all MCP targets along with the megamaser system in NGC 4258

Using the distance and velocity measurements from the maser modeling, we have fit a simple cosmological model and constrained the Hubble constant to  $H_0 = 73.9 \pm 3.0$  km/s/Mpc

- This constraint assumes a peculiar velocity uncertainty of 250 km/s associated with each galaxy
- Alternative peculiar velocity mitigation strategies have modest ( $<1\sigma$ ) impacts

Future MCP  $H_0$  constraints will incorporate distance measurements from additional megamaser-hosting galaxies

Substantial improvements beyond the current precision will likely require new observational tools

- e.g., (sub)mm transitions and next-generation facilities

Additional slides

We parameterize warping in both the position angle and inclination directions using polynomial expansions in orbital radius,

$$i(r) = i_0 + i_1 r + \frac{1}{2} i_2 r^2$$

$$\Omega(r) = \Omega_0 + \Omega_1 r + \frac{1}{2} \Omega_2 r^2$$

Model velocities incorporate special and general relativistic effects, and these are combined with cosmological motion in redshift space,

$$1 + z = (1 + z_D) (1 + z_g) (1 + z_0)$$

During  $H_0$  fitting, peculiar motions are incorporated in an analogous manner,

$$1 + \hat{z}_i = (1 + z_i) \left( 1 + \frac{v_{\text{pec},i}}{c} \right)$$

When fitting maser disk models, we work with three classes of measurements:

- positions (x,y)
- velocities (v)
- accelerations (a)

Each of these measurements has an associated systematic uncertainty that we quantify using an “error floor” term in the likelihood. E.g., for the acceleration likelihood,

$$\ln(\mathcal{L}_2) = -\frac{1}{2} \sum_k \left[ \frac{(a_k - A_k)^2}{\sigma_{a,k}^2 + \sigma_a^2} + \ln[2\pi(\sigma_{a,k}^2 + \sigma_a^2)] \right]$$

The primary recent improvements to the maser distance measurements come from treating these error floors as free parameters in the modeling

- We have found that previous MCP estimates for the calibration uncertainty associated with maser spot position measurements had been too conservative (i.e., the error floors were systematically overestimated)
- For the high-SNR maser systems in which systematics dominated the uncertainty (i.e., NGC 4258 and NGC 5765b), the error floor modeling has significantly improved the distance measurements (factor of ~2 decrease in uncertainty)

# Leave-one-out jackknife tests



We investigated the effect on our  $H_0$  constraints when removing each galaxy from the sample (for each different peculiar velocity treatment), and we find that no single galaxy dominates the total constraint

- deviations from full-fit value are always below  $1\sigma$  when removing a single galaxy
- upward and downward deviations seem to be comparably represented and have comparable magnitudes

Peculiar Velocity Treatment	Galaxies Excluded from the Fit	$H_0$ ( $\text{km s}^{-1} \text{Mpc}^{-1}$ )
(1) Assign a fixed velocity uncertainty of $250 \text{ km s}^{-1}$	UGC 3789	$75.8^{+3.4}_{-3.3}$
	NGC 6264	$73.8^{+3.2}_{-3.2}$
	NGC 6323	$73.8^{+3.1}_{-3.0}$
	NGC 5765b	$74.1^{+4.5}_{-4.4}$
	CGCG 074-064	$72.5^{+3.4}_{-3.2}$
	NGC 4258	$73.6^{+3.1}_{-3.0}$
	Fit using all galaxies:	$73.9^{+3.0}_{-3.0}$
(2) Fit for $\sigma_{\text{pec}}$ using the maser data and assuming an outlier-robust form for the peculiar velocity distribution	UGC 3789	$76.4^{+4.2}_{-3.8}$
	NGC 6264	$74.4^{+4.4}_{-3.8}$
	NGC 6323	$74.5^{+4.0}_{-3.6}$
	NGC 5765b	$75.8^{+6.6}_{-5.6}$
	CGCG 074-064	$73.1^{+4.3}_{-3.9}$
	NGC 4258	$74.2^{+4.5}_{-3.7}$
	Fit using all galaxies:	$74.4^{+3.9}_{-3.4}$
(3) Use galaxy group recession velocities	UGC 3789	$75.0^{+3.1}_{-3.0}$
	NGC 6264	$73.1^{+2.8}_{-2.7}$
	NGC 6323	$73.2^{+2.8}_{-2.7}$
	NGC 5765b	$72.2^{+4.2}_{-4.1}$
	CGCG 074-064	$73.3^{+3.1}_{-3.0}$
	NGC 4258	$72.8^{+2.8}_{-2.7}$
	Fit using all galaxies:	$73.3^{+2.8}_{-2.7}$

Peculiar Velocity Treatment	Galaxies Excluded from the Fit	$H_0$ ( $\text{km s}^{-1} \text{Mpc}^{-1}$ )
(4) Use 2M++ (Carrick et al. 2015) recession velocities	UGC 3789	$73.3^{+3.0}_{-3.0}$
	NGC 6264	$71.8^{+2.8}_{-2.8}$
	NGC 6323	$71.9^{+2.8}_{-2.7}$
	NGC 5765b	$71.1^{+4.0}_{-3.9}$
	CGCG 074-064	$70.9^{+3.0}_{-2.9}$
	NGC 4258	$72.1^{+2.7}_{-2.7}$
	Fit using all galaxies:	$71.8^{+2.7}_{-2.7}$
(5) Use CF3 (Graziani et al. 2019) recession velocities	UGC 3789	$73.6^{+3.1}_{-2.9}$
	NGC 6264	$71.5^{+2.8}_{-2.7}$
	NGC 6323	$71.7^{+2.8}_{-2.6}$
	NGC 5765b	$71.5^{+4.1}_{-4.0}$
	CGCG 074-064	$70.5^{+3.0}_{-2.9}$
	NGC 4258	$72.0^{+2.7}_{-2.7}$
	Fit using all galaxies:	$71.8^{+2.7}_{-2.6}$
(6) Use M2000 (Mould et al. 2000) recession velocities	UGC 3789	$79.3^{+3.3}_{-3.1}$
	NGC 6264	$76.8^{+2.9}_{-2.9}$
	NGC 6323	$76.9^{+2.9}_{-2.9}$
	NGC 5765b	$76.2^{+4.3}_{-4.1}$
	CGCG 074-064	$75.5^{+3.2}_{-3.0}$
	NGC 4258	$76.8^{+2.9}_{-2.9}$
	Fit using all galaxies:	$76.9^{+2.9}_{-2.9}$

Table 2 from Pesce et al. (2020b)

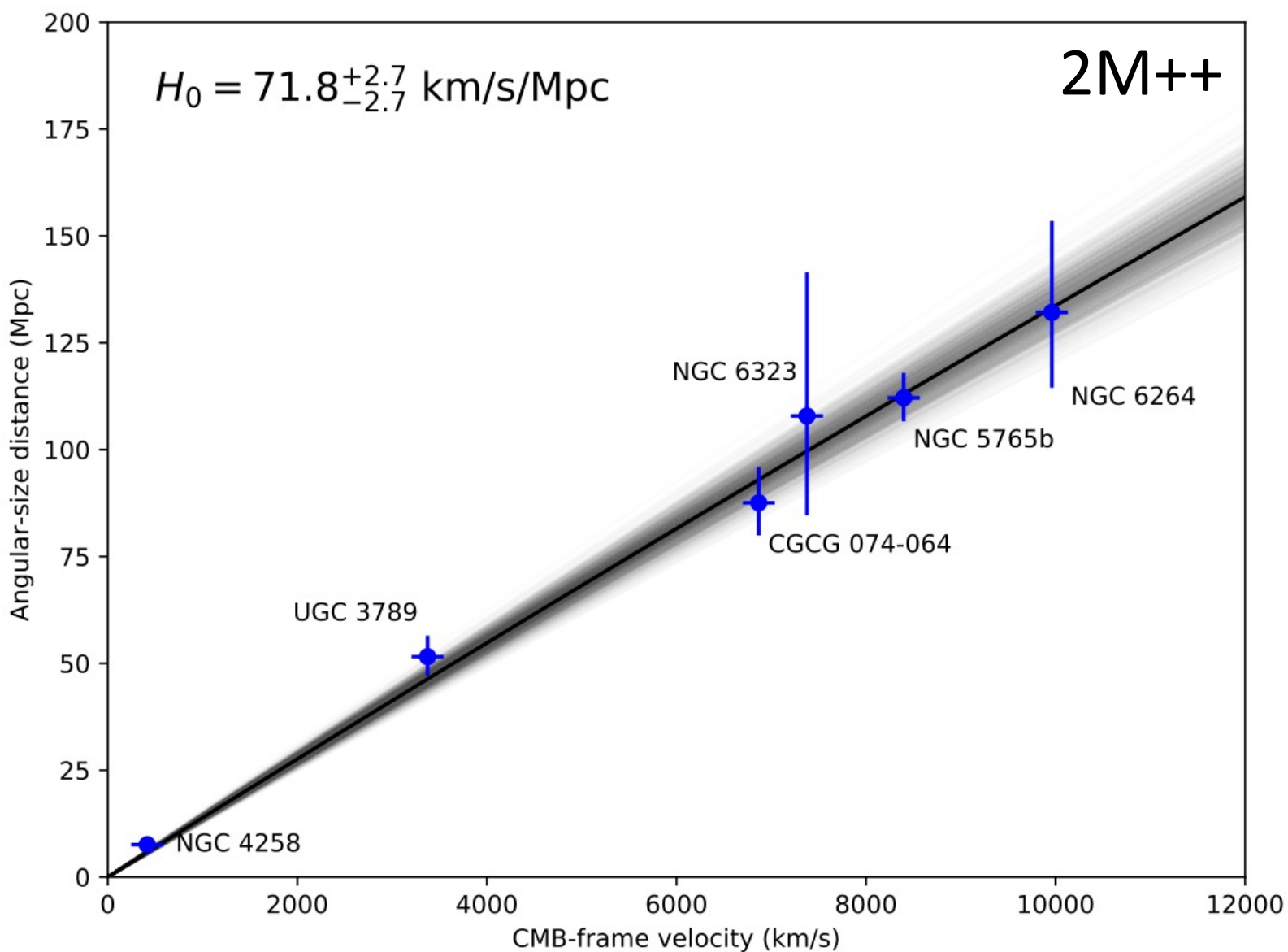


# 2M++ versus CF3 peculiar velocity corrections



Taken at a glance, both the 2M++ and the CF3 peculiar velocity corrections appear to produce nearly identical  $H_0$  constraints, which might argue in favor of their robustness

A closer look reveals that this alignment seems to be happenstance, as the specific corrections for each galaxy are quite disparate between the two catalogs

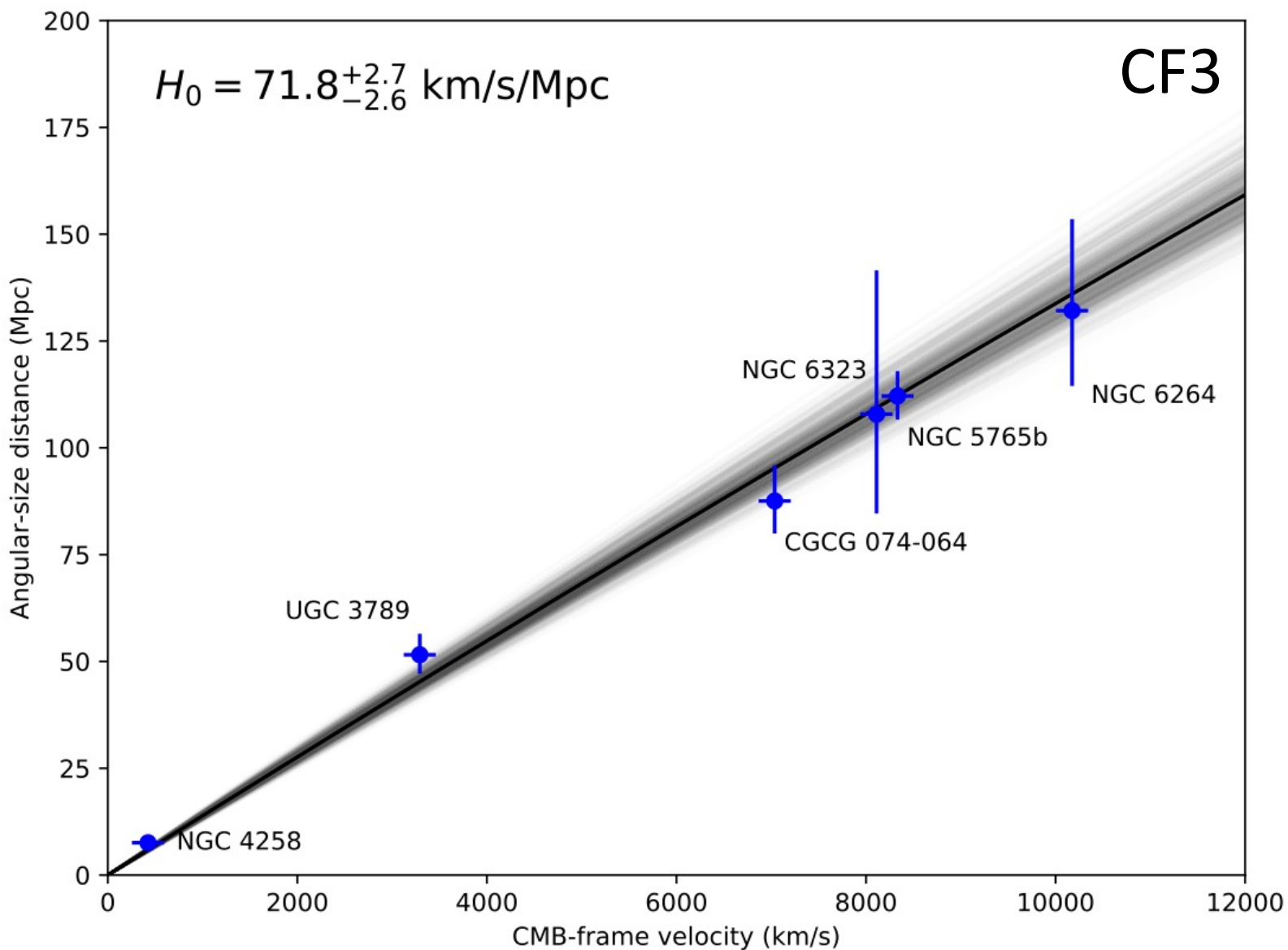


# 2M++ versus CF3 peculiar velocity corrections



Taken at a glance, both the 2M++ and the CF3 peculiar velocity corrections appear to produce nearly identical  $H_0$  constraints, which might argue in favor of their robustness

A closer look reveals that this alignment seems to be happenstance, as the specific corrections for each galaxy are quite disparate between the two catalogs



In practice, we use

$$D_i = \frac{c}{H_0(1+z_i)} \int_0^{z_i} \frac{dz}{\sqrt{\Omega_m(1+z)^3 + (1-\Omega_m)}}$$
$$\approx \frac{cz_i}{H_0(1+z_i)} \left( 1 - \frac{3\Omega_m z_i}{4} + \frac{\Omega_m(9\Omega_m - 4)z_i^2}{8} \right)$$

to translate between distances/redshifts and  $H_0$ . The approximation is good to a part in  $10^5$  for our targets.

We set  $\Omega_m = 0.315$  from Planck Collaboration et al. (2018), but any value in the range (0,0.5) would yield a distance that differs by <1% for the galaxies in our sample.